Stationary Phase Analysis of the Seismic Interferometry Applied to Dipping Reflectors

Antonio J. Ortolan Pereira (Petrobras/E&P/EXP & FEM/University of Campinas) and Ricardo Biloti (IMECC/University of Campinas & INCT-GP)

Abstract

Seismic Interferometry is a relative new branch of Seismic and Seismology. Despite the start with paper of Claerbout (1968), it was only during the late nineties that the use of Seismic Interferometry start continuously increasing in Seismic. One of the most promising use of this technique is the ability to create new positions of sources and receivers by crosscorrelating the seismic wavefield recorded. To understand the physical meaning of Seismic Interferometry we study one of its fundamental equations by means of the Stationary Phase method, in a very simple geometry: a flat dip reflector.

Introduction

In a not rigorous definition it is possible to define Seismic Interferometry as a variety of methods used to create virtual seismograms, never physically recorded. These virtual seismograms are created only through mathematical operations, which include crosscorrelating, convolution, deconvolution and summation of actually recorded wavefields, Galetti and Curtis (2012). One of the most interesting applications of interferometric methods is the ability to produce artificially traces in positions of sources or receivers that are not possible to be located. With this capacity, at least in principle, it is possible to fill gaps in seismic acquisition (Interferometric Interpolation, Wang et al. (2009)). This possibility is a direct consequence of the nature of physical process behind Seismic Interferometry, which is clarified by Stationary Phase method.

Seismic Interferometry

The retrieval of the Green's Function, or the response of a given media when excited by an impulsive source, is made with interferometric reciprocity equation of correlation type by equation 1 (Wapenaar, 2004; Schuster, 2009), given by

$$\Im \hat{G}(\mathbf{x}_B,\omega;\mathbf{x}_A) = -\omega \oiint_{\varepsilon} \frac{1}{c(x)} \hat{G}(\mathbf{x}_A,\omega;\mathbf{x}) \hat{G}^*(\mathbf{x}_B,\omega;\mathbf{x}) d\mathbf{S}, \quad (1)$$

where $\Im$ denotes the imaginary part, $\hat{G}(\mathbf{x}_B,\omega;\mathbf{x}_A)$ is the Fourier Transform of the Green's Functions for a source at $\mathbf{x}_A$, evaluated at a receiver at $\mathbf{x}_B$, and ω is the frequency, $\hat{G}^*$ is its complex conjugate, $\mathbf{x}$, the variable of integration, represents source positions over the surface ε, $d\mathbf{S}$ is the element of area, and $c(\mathbf{x})$ is the velocity. The positions $\mathbf{x}_A$ and $\mathbf{x}_B$, where the Green's Functions is computed are located inside the volume bounded by surface ε. All those elements are sketched on Figure 1.

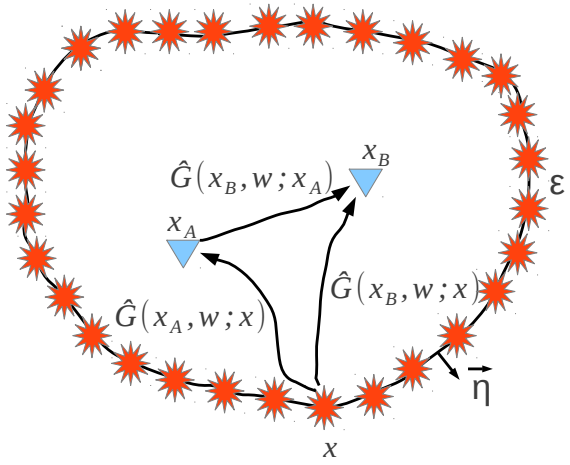

Figure 1: In the figure the rays represent the full responses between the source and receivers points, including primary and multiples due to inhomogeneities inside and outside volume (based on Wapenaar and Fokkema (2006)).

By means of equation (1), a primary reflection from $\mathbf{x}_A$ to $\mathbf{x}_B$ can be obtained by crosscorrelating multiple and primary reflections acquired in the field. This is illustrated through a ray diagram, in marine seismic, in the figure below. In this specific example the dominant arrivals are assumed to be the reflection primaries and free-surface first order multiples. The direct arrivals are muted in the data, an easy task in depth marine seismic. The Green's function can be approximated as a sum of specular primary reflection and first order multiple reflection. The crosscorrelation of primaries and primaries or multiples and multiples do not contribute significantly, because as we shall see the stationary contributions of these terms is zero. For a constant velocity overburden, $c(\mathbf{x}) = v$, the Green's Function accounting only for primaries and first order multiples is asymptotically approximated by

$$\hat{G}(\mathbf{x}_M,\omega;\mathbf{x}) \approx \overbrace{r_M \frac{\exp(-i\omega T_{\mathbf{x}\mathbf{x}_M})}{4\pi v T_{\mathbf{x}\mathbf{x}_M}}}^{Primary} + \overbrace{r'_M \frac{\exp(-i\omega \mathit{TT}_{\mathbf{x}\mathbf{x}_M})}{4\pi v \mathit{TT}_{\mathbf{x}\mathbf{x}_M}}}^{Multiple}, \quad (2)$$

where r_M and r'_M are the reflection coefficients associated to the primary and multiple reflections, the traveltimes for specular primary reflection and first order free-surface

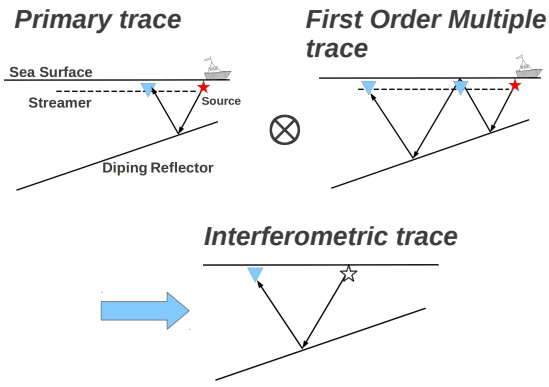

Figure 2: Diagram of crosscorrelating primaries and multiples from a dipping reflector, modified from Wang et al. (2009). The cross correlation of a primary and a first order multiple results in an interferometric trace.

multiple are $T_{\mathbf{x}\mathbf{x}_M}$ and $\mathcal{T}_{\mathbf{x}\mathbf{x}_M}$, respectively, for source in $\mathbf{x}$, and receiver in $\mathbf{x}_M$ at marine surface.

Replacing the expression for Green's Function of equation 2 into 1,

$$\Im\hat{G}(\mathbf{x}_B,\omega;\mathbf{x}_A) \approx -\frac{\omega}{v} r_M r'_M \int_{S_0} \frac{\exp\{-i\omega(\mathcal{T}_{\mathbf{x}\mathbf{x}_B} - T_{\mathbf{x}\mathbf{x}_A})\}}{(4\pi)^2 \mathcal{T}_{\mathbf{x}\mathbf{x}_B} T_{\mathbf{x}\mathbf{x}_A}} d\mathbf{S} + \mathbf{O.T.}, \quad (3)$$

where O.T. stands for higher order terms, called *virtual multiples* or cross talk, and will be attenuated in the final image for a sufficient large integration's aperture. A last approximation made in equation 3 was to consider that the integral over S_∞ vanishes as its ray goes to infinity. The Figure 3 shows the geometry for this integral.

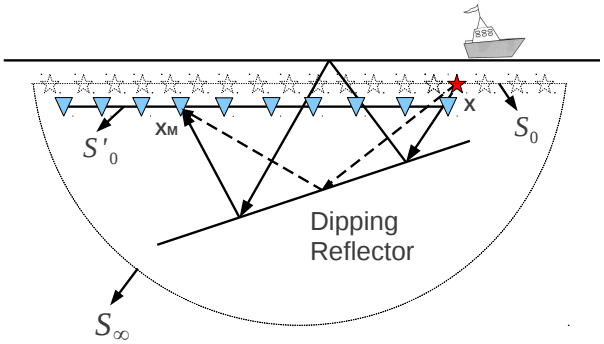

Figure 3: Geometry and surface of integration of equation 3, based on Schuster (2009).

Since the integrand in equation 3 has an oscillatory character the integral can be asymptotically estimated by the Stationary Phase method (Bleistein, 1984).

Stationary Phase

The stationary phase method is a method to obtain an asymptotically approximation for integral with an oscillatory term of the form

$$I = \int_{-\infty}^{\infty} F(x)\, e^{i\omega\phi(x)}\, dx, \quad (4)$$

where ϕ is a rapid varying function of x over most range of integration, and F is a slowly waring function of x. Such kind of integrals frequently arise in radiation and scattering problems. Due to the rapid variation of exponential term the integral is approximately zero over all ranges of ω, except at regions where $\phi'(x) \approx 0$. Each x^* such that $\phi'(x^*) = 0$, is called an *stationary point* of ϕ. Bleistein (1984) shows that I can be fairly approximated as

$$I \sim \sqrt{\frac{2\pi}{\omega|\phi''(x^*)|}} F(x^*)\, e^{(i\omega\phi(x^*) + i\omega\pi/4)}. \quad (5)$$

This formula says that dominant contribution to the integral comes from point(s) where phase is stationary.

Stationary Phase method in a Presence of a Dipping Reflector

The use Stationary Phase method to interpret the Seismic Interferometric results in the case of horizontal reflectors was done by Snieder (2004), Snieder et al. (2006), and recently by Draganov et al. (2012).

Following the same strategy, we also employ the Stationary Phase method to investigate if, in the presence of a dipping reflector in a medium of constant velocity, the seismic interferometric interpolation can be useful to create virtual traces.

In our case, the phase function $\phi(x) = \mathcal{T}(x,x_B) - T(x,x_A)$, where x, x_A, and x_B are the horizontal coordinate of points $\mathbf{x}$, $\mathbf{x}_A$, and $\mathbf{x}_B$, respectively, since we are only dealing with 2D acquisition lines. Note that both traveltimes are from source at x. Therefore, it would be more suitable to work with traveltime formulas for common shot configurations.

For primary reflections traveltime we will use an expression similar to the one presented on Sheriff and Geldart (1995), pp. 87. To simplify the notation use $T_{x,h}$ to represent the traveltime of a primary reflection from a source at x to a receiver at $2h$ ahead.

$$T_{x,h} = T_0(x)\sqrt{1 + \frac{h^2 + 2hd(x)\sin\alpha}{d^2(x)}}, \quad (6)$$

where $T_0(x)$ is the traveltime of the zero-offset reflection from the source in x, h is the half-offset, $d_1(x)$ is normal distance from the source to the reflector, α is the dip angle. The zero-offset travelime and normal distance vary with x as

$$T_0(x) = \frac{2z(x)\cos\alpha}{v} \quad (7)$$

and

$$d(x) = z(x)\cos\alpha, \quad (8)$$

where $z(x)$ is the depth of the dip reflector at x

$$z(x) = z_0 + (x - x_0)\tan\alpha, \quad (9)$$

form some fixed point (x_0, z_0) over the reflector (see Fig. 4).

The traveltime of a multiple reflection, in such geometry, is equal to the traveltime of a primary reflection at a double dip

reflector. Therefore, the same expressions just presented by the primary-reflection traveltime can be recasted for the multiple-reflection traveltime:

$$\mathcal{T}_{x,h} = \hat{T}_0(X)\sqrt{1+\frac{h^2+2h\hat{d}(x)\sin 2\alpha}{\hat{d}^2(x)}}, \tag{10}$$

where

$$\hat{T}_0(x) = \frac{2\hat{z}(x)\cos 2\alpha}{v}, \tag{11}$$

and

$$\hat{d}(x) = \hat{z}(x)\cos 2\alpha, \tag{12}$$

where $\hat{z}(x)$ is the depth of the virtual double-dip reflector

$$\hat{z}(x) = \hat{z}_0 + (x - x_0)\tan 2\alpha, \tag{13}$$

with $\hat{z}_0 = z_0(\cos 2\alpha + \sin 2\alpha \tan 2\alpha)$.

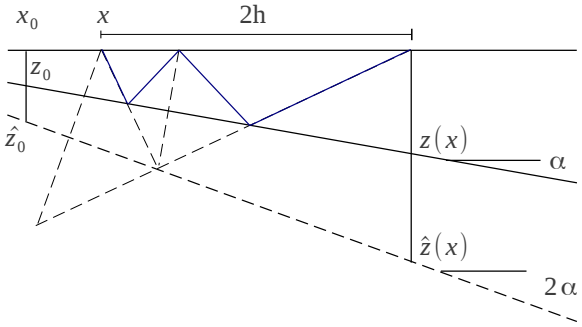

Figure 4: Geometry for the primary and multiple events in Equations 6 and 13.

From equation (3), the function ϕ, for the stationary phase method, is given by

$$\phi(x) = \mathcal{T}_{x,h} - T_{x,h}. \tag{14}$$

To find the stationary points, representing the sources that contribute most to the integral 3, we just have to solve the equation

$$\frac{d\phi(x)}{dx} = 0. \tag{15}$$

Results

It is not possible to solve the expression in equation 15 analytically. However, it is fairly simple to solve it numerically. We present two tests simulating a 2D acquisition line, one for shallow water and another for deeper water. The example with shallow water one receiver, x_A, is located above 200 m of a flat reflector with 10° dip. The other receiver, x_B, is located at a distance of 1000 m of the first one, x_A, downdip. For this two receivers there is only one stationary point x^* at a distance of 292.76 m in shallow water of x_A. Figure 5 shows the situation.

The second example is a deep water environment with x_A located above 1000 m of the same 10° dip reflector. The other receiver, x_B, is locate at the same distance of the first one (separation of 1000 m). Again, for this configuration there is only one stationary point x^* at a distance of 161.34 m of x_A (see Fig. 6).

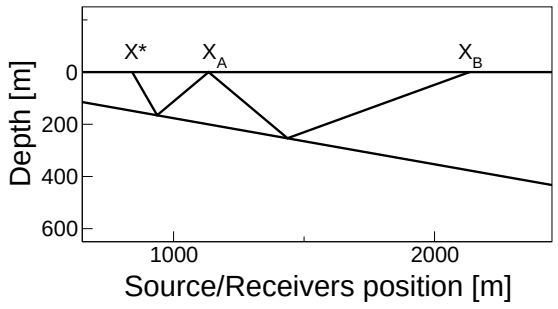

Figure 5: In this shallow water example one receptor is located at 200 m above a dip reflector (10° dip). The stationary point is 292.76 m of x_A. The distance between x_A and x_B is 1000 m.

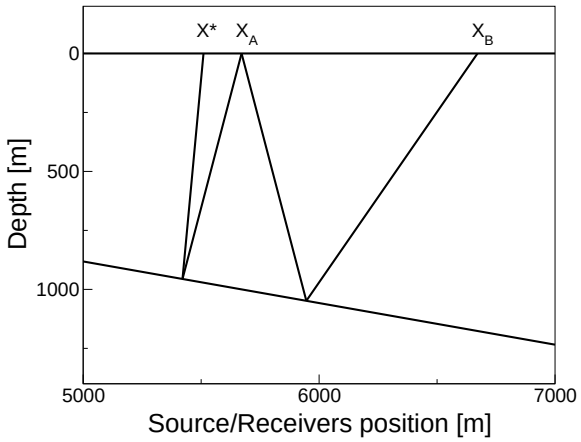

Figure 6: In deep water, one receptor is locate at 1000 m above the same flat dip reflector. The stationary point is only 161.34 m of x_A, updip direction.

To investigate how the stationary point moves as the distance of x_A and x_B varies, we present to further results in figures 7 and 8. The horizontal axis is the distance that separates x_A and x_B. x_A was kept fixed, while x_B was shifted from x_A position up to 12 km, downdip. The vertical axis is the relative position of the stationary point to the x_A receiver, $(x^* - x_A)$, i.e., negative values stand for a stationary points at right of x_A, while positive values stand for stationary points at left of x_A.

In the deep water we can observe, for some stationary points between the positions of the two receptors (points above the horizontal line in Figure 8).

Conclusions

From the experiments we have made, we can observe that in the shallow water situation the range of practical applicability of the Seismic interferometric approximation for primary reflection traces is limited. From Figure 7 we see that to simulate traces with small offsets it would be necessary sources too near to x_A, which is in principle a location where no source was fired. Furthermore, in typical range of offsets for shallow water, let say from 250 m up

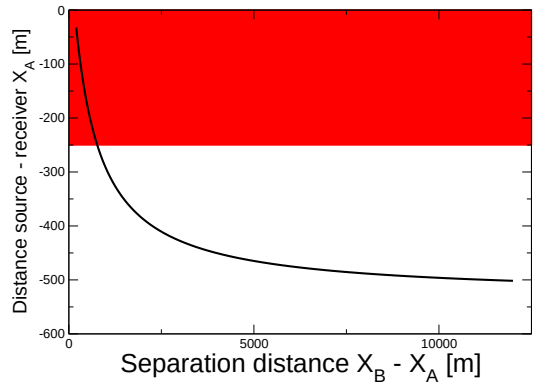

Figure 7: Relative position of the stationary point in the shallow water case.

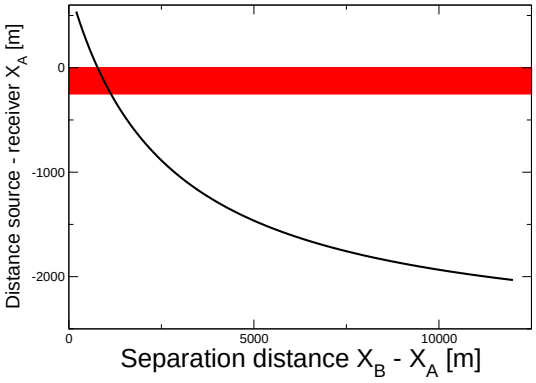

Figure 8: Relative position of the stationary point in the deep water case.

to 4 km, the same figure shows that the stationary points cover a narrow interval from x_A up to around 450 m to x_A, downdip. The red strip in the figure indicates the range of offsets between sources and x_A which are not present in the data. In the usual acquisition geometry this means at most 11 shot points, with 25 m between consecutive shots, would be available. The first trace feasible to be recovered by interferometric formula 3 is the one with offset 775 m.

In the case of deep water, from Figure 8, we see that the range of positions for stationary points is more favorable, varying from 250 m up to 1930 m, for very long cables. In this range, there is typically 67 shots. Note also, that in this scenario, for small offset it would be necessary sources between the receivers in x_A and x_B, which is highly uncommon to happen in an end-on conventional acquisition geometry. Again, the red strip in the figure indicates the range of offsets between sources and x_A which are not present in the data. The first trace feasible to be recovered by interferometric formula 3 is the one with offset 1130 m.

Using stationary-phase method's approach and with the simple geometry of a dip reflector, we were able to investigate what are the spatial conditions to create new sources with Seismic Interferometry. It should also be investigated the dependence on the dip angle.

References

Bleistein, N., 1984, Mathematical methods for wave phenomena: Academic Press Inc. (Harcort Brace Jovanovich Publishers).

Claerbout, J. F., 1968, Synthesis of layered medium from its acoustic transmission response: Geophysics, **33**, 264–269.

Draganov, D., K. Heller, and R. Ghose, 2012, Monitoring CO2 storage using ghost reflections retrieved from seismic interferometry: International Journal of Greenhouse Gas Control, **11**, S35–S46.

Galetti, E. and A. Curtis, 2012, Generalised receiver functions and seismic interferometry: Tectonophysics, **532-535**, 1–26.

Schuster, G. T., 2009, Seismic interferometry: Cambridge University Press.

Sheriff, R. E. and L. P. Geldart, 1995, Exploration seismology, 2nd ed.: Cambridge University Press.

Snieder, R., 2004, Extracting the Green's function from the correlation of coda waves: A derivation based on stationary phase: Physical Review E, **69**, 046610.

Snieder, R., K. Wapenaar, and K. Larner, 2006, Spurious multiples in seismic interferometry of primaries: Geophysics, **71**, SI111–SI124.

Wang, Y., Y. Luo, and G. Schuster, 2009, Interferometric interpolation of missing data: Geophysics, **74**, SI37–SI45.

Wapenaar, K., 2004, Retrieving the elastodynamic Green's function of an arbitrary inhomogeneous medium by cross correlation: Physical Review Letters, **93**, 254301–1–254301–4.

Wapenaar, K. and J. Fokkema, 2006, Green's function representations for seismic interferometry: Geophysics, **71**, SI33–SI46.

Acknowledgments

This work was kindly supported by the Brazilian agencies CAPES, FINEP, and CNPq, as well as Petrobras and the sponsors of the *Wave Inversion Technology (WIT) Consortium*.